

Document downloaded from:

<http://hdl.handle.net/10251/166737>

This paper must be cited as:

Gasque Albalate, M.; González Altozano, P.; Gutiérrez-Colomer, RP.; García-Marí, E. (2020). Optimisation of the distribution of power from a photovoltaic generator between two pumps working in parallel. *Solar Energy*. 198:324-334.  
<https://doi.org/10.1016/j.solener.2020.01.013>



The final publication is available at

<https://doi.org/10.1016/j.solener.2020.01.013>

Copyright Elsevier

Additional Information

1 OPTIMISATION OF THE DISTRIBUTION OF POWER FROM A PHOTOVOLTAIC  
2 GENERATOR BETWEEN TWO PUMPS WORKING IN PARALLEL

3

4 María Gasque<sup>a</sup>, Pablo González-Altozano<sup>b,\*</sup>, Rosa Penélope Gutiérrez-Colomer<sup>b</sup>, Eugenio  
5 García-Marí<sup>b</sup>

6 <sup>a</sup> *Dept. Física Aplicada, Universitat Politècnica de València, Camino de Vera s/n, 46022*  
7 *Valencia, Spain*

8 <sup>b</sup> *Dept. Ingeniería Rural y Agroalimentaria, Universitat Politècnica de València, Camino de*  
9 *Vera s/n, 46022 Valencia, Spain*

10

11 **Abstract**

12 In this work, a method for distributing the power generated in a photovoltaic pumping system  
13 equipped with two equal pumps, working in parallel is analysed.

14 For this purpose, a system equipped with two pumping groups 0.75kW each was  
15 investigated. Experimental tests at five different working frequencies (30 to 50 Hz), and at six  
16 pumping heads (18 to 48 m) were carried out.

17 The main objective of this paper is to establish a strategy for the distribution of the generated  
18 power that maximises the flow rate from the set of two pumps. This distribution depends both  
19 on the available electric power and on the pumping head.

20 The results show some differences between higher and lower pumping heads, but in both  
21 cases for lower power values, the strategy involves the operation of a single pump with the  
22 limitation that the power assigned to this pump cannot exceed the maximum value ( $P_{max}$ ).  
23 However, if the available power exceeds a certain value, referred to as  $P_e$ , it must then be  
24 distributed at 50% between the two pumps. Thus, there is no power distribution ratio other  
25 than 0 and 50% that maximises the flow rate, except that required to limit the power assigned  
26 to one of the pumps to  $P_{max}$ .

27 It was proven that the optimal distribution strategy for the available power depends on  
28 whether  $P_e > P_{max}$  (for higher pumping heads) or  $P_e < P_{max}$  (in case of lower heads). In practice,  
29 it is easy to determine which case applies using a simple pumping test.

30

31 **Keywords:** pumping system; power optimisation; multi-pump system; parallel pumps

32

33 **Nomenclature**

34  $H_{\max}$  (m): Maximum pumping head at nominal speed

35  $k$ : Distribution ratio of the available electric power between the two pumps

36  $k_{\min}$ : Minimum value of  $k$  in a given power range

37  $k_{\text{opt}}$ : Optimal power distribution ratio between the two pumps.

38  $P$  (kW): Electric power supplied to the motor-pump group

39  $P_e$  (kW): Power value above which the two pumps operate with power distribution at 50%

40  $P_h$  (kW): Hydraulic power

41  $P_{\max}$  (kW): Maximum motor-pump power

42  $P_{\min}$  (kW): Minimum power to start pumping

43  $q(P)$  (L/s): Flow rate propelled by one pump

44  $Q(P)$  (L/s): Flow rate propelled by the two pumps operating in parallel.

45

46 *Greek symbol*

47  $\eta_{\text{mp}}$ : Efficiency of motor-pump group

48

## 49 **1. Introduction**

50 Photovoltaic (PV) pumping systems have proved to be an alternative method of supplying  
51 drinking water for human consumption. They also play an important role as a sustainable  
52 alternative for the agricultural sector. The applications of greatest interest are in remote rural  
53 areas of developing countries with high annual irradiance levels, where grid electricity is not  
54 easily available (Alonso, 2005; Meah et al., 2008; Aliyu et al., 2018; Wazed et al., 2018).

55 Solar pumping systems have also become widely used to supply electricity to the pumping  
56 facilities necessary for the irrigation of many crops e.g. in Latin America (Fedrizzi and Sauer,  
57 2002; Espericueta et al., 2004; Guzmán et al., 2018), in Asia (Shoeb and Shafiullah, 2018),  
58 as well as in many countries of the Mediterranean region (López-Luque et al., 2015; García-  
59 Tejero and Durán-Zuazo, 2018; Narvarte et al., 2018; Todde et al., 2019).

60 In these facilities, the high variability of the incident solar radiation results in irregular electric  
61 power generation over time, meaning that the pump operates at variable flow rates  
62 (Hamrouni et al., 2009; Campana et al., 2013; Benghanem et al., 2018; Tiwari and Kalamkar,  
63 2018).

64 In order to maximise the energy utilisation and to avoid to the extent as possible the effect of  
65 weather and irradiance fluctuations on the efficiency of pumping system, many solutions  
66 have been reported in the literature. It is worth noting some of them. Thus, Mérida García et  
67 al. (2018) developed an irrigation management model which enables synchronizing the PV  
68 energy production with the pumping power demand and also compensates occasional water  
69 supply lacks due to irradiance fluctuations. An optimisation approach based on the  
70 application of technical solutions to the design and implementation of a hybrid PV-diesel  
71 irrigation system was presented in Almeida et al. (2018a). These solutions were developed to  
72 overcome the PV peak power due to the passing clouds and to the imbalance between PV  
73 production and water needs. Almeida et al. (2018b) reduced power threshold to start  
74 pumping achieving longer periods of pumping. They proposed a pump selection method  
75 based on considering the efficiency in the whole range of operating frequencies. In Matam et  
76 al. (2018), a novel Reconfigurable PV Array based water pumping scheme is proposed to  
77 improve the response under various operating conditions. In the case of PV pumping  
78 systems based on a three phase induction motor without storage elements, Talbi et al.  
79 (2018) proposed an scheme which resulted in more pumped water under variable pumping  
80 heads, whereas Elkholy and Fathy (2016) developed an Artificial Neural Network model to  
81 obtain the optimal inverter voltage and frequency to extract maximum power from the PV  
82 array.

83 In conventional pumping stations, it is common to use various pumps working in parallel,  
84 which increases energy savings and enlarge the range of achieved flow rate with raised  
85 efficiency (Kaya et al., 2008; Pemberton and Bachmann, 2010; Koor et al., 2016). In this  
86 context, several researchers have developed different control methods and strategies which  
87 result very useful in optimising pumping efficiency (Shankar et al., 2016). In PV systems, this  
88 operating mode allows for the pumps to start at lower irradiance levels.

89 In PV facilities with several pumps working in parallel, it is possible to install an independent  
90 PV generator for each pump. Another option is to use a single PV generator to supply the  
91 entire facility, and to establish either a strategy of equal distribution of the generated power

92 among the different pumps or a more efficient distribution strategy that allows for optimisation  
93 of the flow rate pumped by the facility at any time.

94 The aim of this work is to establish a strategy for the distribution of the power generated in a  
95 PV pumping system equipped with two equal submersible motor-pump groups, working in  
96 parallel, to maximise the flow rate pumped. The motor-pump groups are fed by means of a  
97 single PV generator through frequency converters. Both groups have the same dynamic  
98 water level, and work in parallel on the same hydraulic network.

99 In order to achieve this objective, laboratory trials were performed to determine the flow-head  
100 and flow-power characteristic curves at variable working frequencies and different pumping  
101 heads, thus establishing the flow rate propelled by the pumping group under each set of  
102 working conditions.

103

## 104 **2. Materials and Methods**

### 105 *2.1. Experimental method*

106 A system equipped with two pumping groups 0.75 kW each working in parallel on the same  
107 hydraulic network, was investigated. Experimental tests to determine the flow rate-pumping  
108 head (Q-H) and the flow rate-electric power (Q-P) curves of the pumping group at different  
109 working frequencies were performed in accordance with the international standard IEC  
110 62253:2011.

111 In PV pumping systems, centrifugal and volumetric pumps are predominantly used, being  
112 centrifugal pumps the most common (Benlarbi et al., 2004). A type of pump manufactured by  
113 Bombas Ideal (SKI series) was selected for these experiments. This pump is capable of  
114 pumping at heads of between approximately 18 and 60 m. It is a multistage centrifugal radial-  
115 type submersible pump for boreholes of 4" in diameter. Activation is performed using a three-  
116 phase induction motor of 0.75 kW, at 230 V, 2870 rpm, and 50 Hz (Bombas Ideal catalogue).  
117 In practice, the selection of the pump of a photovoltaic pumping facility must be carried out  
118 taking into account that it works at a variable frequency. Almeida et al. (2018b) proposed a  
119 method for selecting pumps suitable for PV pumping applications based on considering not  
120 only the efficiency at the maximum operating frequency but in the whole range of operating  
121 frequencies.

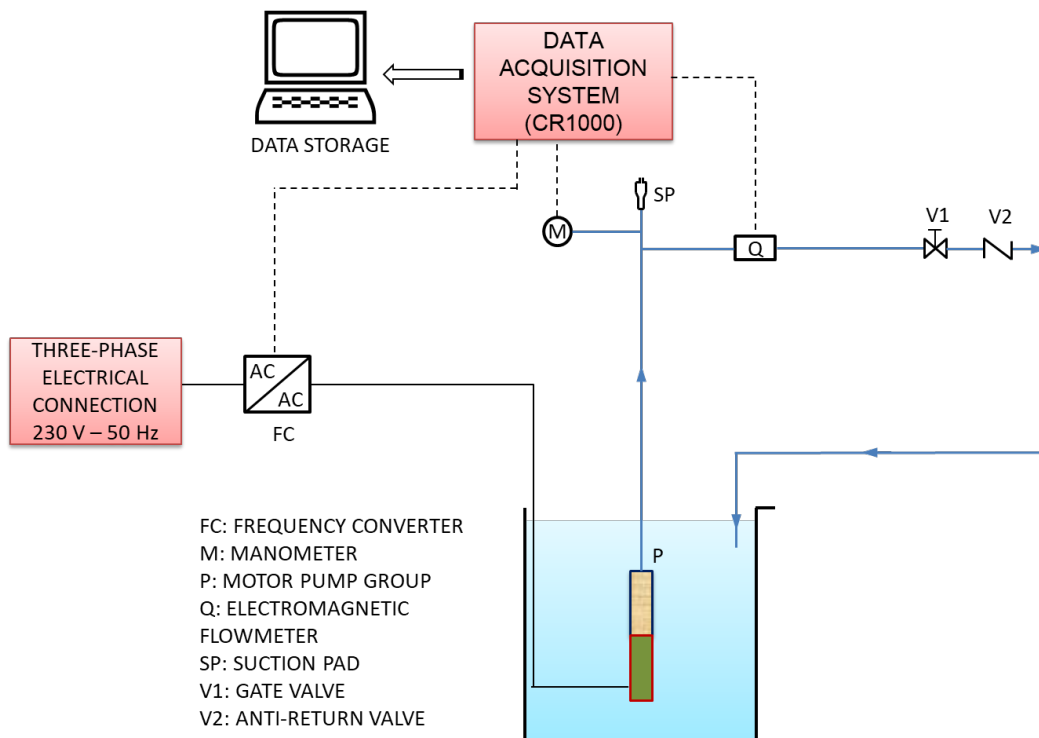
122

### 123 *Experimental setup*

124 The experimental characterisation of the pumping group was carried out in the hydraulic  
125 laboratory at the Universitat Politècnica de València (Spain). Figure 1 shows a schematic  
126 view of the experimental facility.

127 An Altivar 61 (HU30M3 model) was used as a variable speed drive (VSD) to feed the motor-  
128 pump group, allowing modifying the electric power and the flow rate pumped. The VSD  
129 consists of a frequency converter (FC) for three-phase asynchronous motors at 200-240 V  
130 from 0.75 to 3 kW. The frequency of the FC was adjusted by means of a potentiometer  
131 (Alonso et al., 2003). Currently, the FCs used for PV pumping systems are standard  
132 equipment incorporating a solar kit which can operate as an MPPT (Maximum Power Point  
133 Tracker) to track the instantaneous MPP (Maximum Power Point) of the power array. The

134 propulsion pipe of the hydraulic circuit was made of PVC PN10 DN63. The gate valve V1  
 135 allowed modifying and maintaining the head pressure of the pump at a constant value at  
 136 each pumping frequency.



137  
 138 *Figure 1. Schematic view of the experimental setup*

139  
 140 In order to measure the flow rate, an ABB electromagnetic flowmeter was used (model  
 141 FXE4000-DE43) with 50 Hz power supply between 100 and 230 V AC, 4-20 mA electric  
 142 output (accuracy  $\pm 0.5\%$  of rate). A 0.6 bar Wica Eco-Tronic pressure transducer with 4-20  
 143 mA output (accuracy  $\leq 0.5\%$  of span) was used to determine the pressure. The FC provided  
 144 the data acquisition system with the functioning frequency and the electric power supply of  
 145 the motor-pump group. Likewise, every 3 s, the data acquisition system (CR1000 data  
 146 logger, Campbell Scientific) recorded the average values of the data taken from each sensor  
 147 every 0.1 s.

148  
 149 *Flow rate-pumping head characteristic curves (Q-H) at constant frequency*

150 Five Q-H curves for the motor-pump group at frequency intervals of 5 Hz were obtained. The  
 151 frequencies tested were 50, 45, 40, 35 and 30 Hz.

152 At each stage of the trials, the electric power supplied to the motor-pump group from the FC  
 153 was also measured. In this way, the flow-power and flow-efficiency curves of the motor-pump  
 154 group at constant frequency could also be obtained.

155 The efficiency of the motor-pump subsystem ( $\eta_{mp}$ ) was determined as the ratio between the  
 156 hydraulic power  $P_h$  (W) supplied to raise a certain flow rate of water  $Q$  (L/s) to a head  $H$  (m),  
 157 and the electric power  $P$  (W) provided to the pumping group:

158 
$$\eta_{\text{mp}} = \frac{P_h}{P} = \frac{\rho g Q H}{P} \quad (1)$$

159 where  $g$  is the gravitational acceleration ( $\text{m/s}^2$ ) and  $\rho$  is the water density ( $\text{kg/m}^3$ ).

160 Measurements of  $P$  were obtained with the FC, while  $Q$  and  $H$  measurements were obtained  
161 by means of the electromagnetic flowmeter and the pressure transducer respectively.

162

### 163 *Flow rate-electric power characteristic curves (Q-P) at constant head*

164 The characteristic Q-P curves at constant head ( $H$ ) are determined at heads  $H_1=0.3H_{\text{max}}$ ;  
165  $H_2=0.4H_{\text{max}}$ ;  $H_3=0.5H_{\text{max}}$ ;  $H_4=0.6H_{\text{max}}$ ;  $H_5=0.7H_{\text{max}}$ ;  $H_6=0.8H_{\text{max}}$ ; and  $H_7=0.9H_{\text{max}}$  (IEC 62253).  
166  $H_{\text{max}}$  is the maximum pumping head at nominal frequency (50 Hz), which for centrifugal  
167 pumps corresponds to a flow rate of  $Q=0$ .

168 The values of  $Q$  and  $P$  obtained in the experimental trials for each pumping head were  
169 adjusted by regression using a fourth-degree polynomial function:

170 
$$q(P)=a_4 \cdot P^4+a_3 \cdot P^3+a_2 \cdot P^2+a_1 \cdot P+a_0 \quad (2)$$

171 The adjusted equation allows obtaining the flow rate pumped under variable power  
172 conditions and determining the strategy of distribution of the available power  $P$  at each of the  
173 tested heads.

174 From these curves, the minimum power values required to start pumping ( $P_{\text{min}}$ ) were also  
175 obtained at each of the heads tested.

176 In addition to the Q-P curves, the power-efficiency curves at constant head were also  
177 obtained by applying Equation (1).

178

### 179 *2.2. Operation of a PV pumping system with two equal pumps in parallel*

180 In the case of two equal pumps in parallel, two possible ways to design the required PV  
181 generator could be (Figure 2):

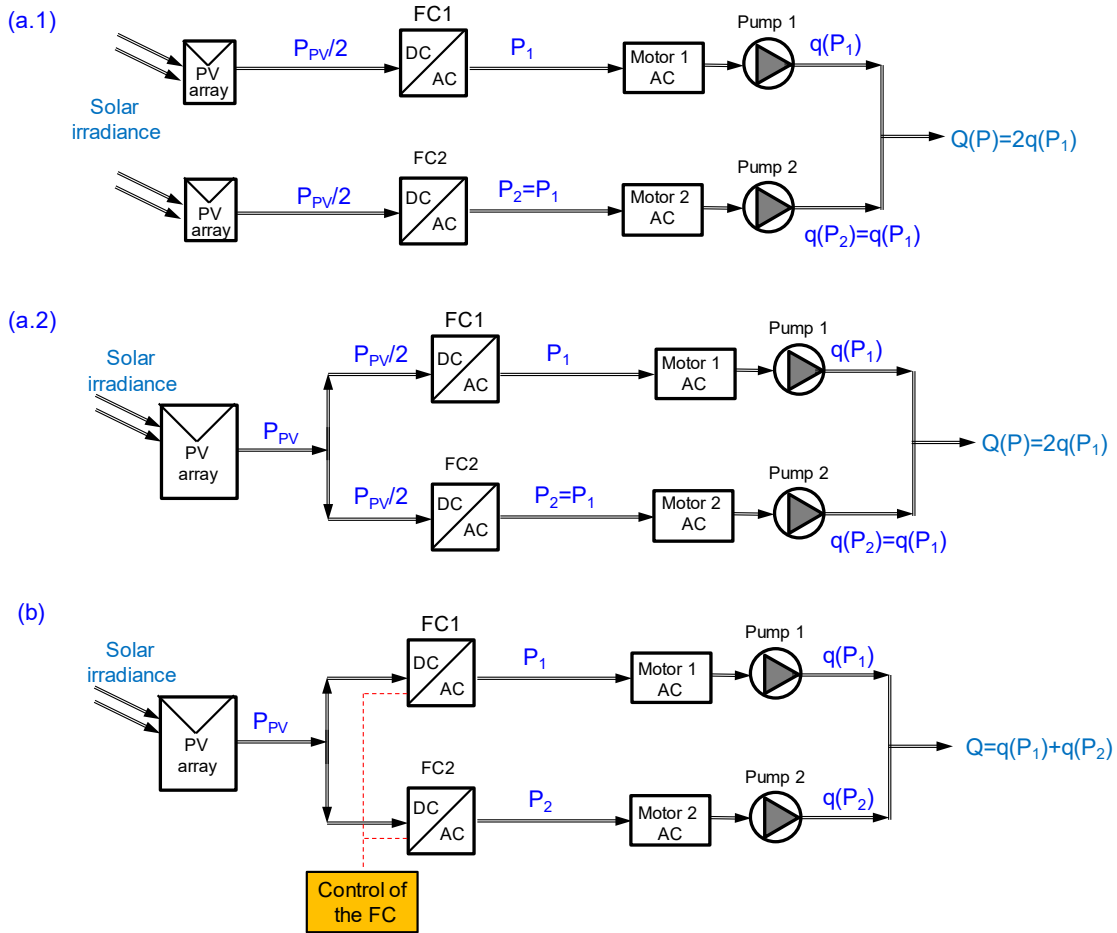
182 (a) Individually for each pump (Figure 2a.1). In this approach, two equal PV generators are  
183 available, and these transfer the electric power generated to their corresponding FC/motor-  
184 pump group. This case is similar to that of a single PV generator (double size of the required  
185 for a single group) where the generated power is distributed in equal amounts (50 %)  
186 between the two FC/motor-pump groups (Figure 2a.2).

187 (b) A single PV generator for both pumps. In this case, the power  $P_{\text{PV}}$  coming from the PV  
188 generator is applied to the pumps via their respective FCs, which can modulate the power  
189 supplied to each pump via the frequency/output voltage control (Figure 2b). This control is  
190 usually done through a PLC (programmable logic controller) which makes one of the FCs the  
191 *master* and the other the *slave*. The *master* is in charge of the MPPT control and the PLC  
192 determines how much power is transmitted to each motor-pump group as well as the power  
193 derived for other uses.

194 In PV pumping systems, there is a pumping threshold irradiance below which the minimum  
195 electric power  $P_{\text{min}}$  is not generated to start the pumping group (Bione et al., 2004). Its value  
196 basically depends on the nominal power of the PV generator and the pumping head. For this

197 reason, the second operating mode can give more favourable results, since it allows a  
 198 suitable power distribution strategy to be adopted, for example at lower solar irradiance  
 199 levels. In this context, when less power is generated, all of it can be assigned to a single  
 200 pump group, thus allowing its operation. In contrast, if the power were distributed at a ratio of  
 201 50 % between the two pumps, neither would not work at low solar irradiance levels, and this  
 202 would cause an increase in the threshold irradiance for pumping.

203 Carrêlo et al. (2020) presented several configurations for large-power PV irrigation systems,  
 204 some of them similar to those described here and shown in Figure 2.



205  
 206 *Figure 2. Design of a PV generator for two motor-pump groups with (a.1) an individual PV generator for each*  
 207 *pump and (a.2) its equivalent with a single PV generator for both pumps, with power distribution ratio 50 %; and*  
 208 *(b) a single PV generator for both pumps with the option to establish a power distribution strategy to maximise the*  
 209 *flow rate.*

210 In order to compare the flow rates pumped in the cases described above, the best power  
 211 distribution strategy in case (b) must be previously investigated.

212

213 **2.2.1. Pumping system with a single PV generator: Distribution of the generated power**  
 214 **between the two pumps**

215 In order to analyse the best distribution strategy for the generated power that allows for  
 216 maximisation of the flow rate provided by the two pumps, a pumping system with two equal  
 217 pumps working in parallel is considered. Equation (2) expresses the relationship between P



218 and  $q$  (flow rate supplied by a single pump) at a certain pumping head, obtained from  
219 experimental tests.

220 When two pumps work in parallel, the power is distributed between them so that  $P=P_1+P_2$   
221 (neglecting the loss in the FC), where  $P_1$  and  $P_2$  represent the electric power feeding pumps  
222 1 and 2 respectively. The flow rates of each pump are (Figure 2b):

$$\begin{aligned} 223 \quad q(P_1) &= a_4 \cdot P_1^4 + a_3 \cdot P_1^3 + a_2 \cdot P_1^2 + a_1 \cdot P_1 + a_0 \\ 224 \quad q(P_2) &= a_4 \cdot P_2^4 + a_3 \cdot P_2^3 + a_2 \cdot P_2^2 + a_1 \cdot P_2 + a_0 \end{aligned} \quad (3)$$

225 For safety reasons, the values of  $P_1$  and  $P_2$  are limited so that they always remain below a  
226 maximum ( $P_{\max}$ ), the value of which only depends on the nominal power of the motor-pump  
227 group.

$$228 \quad P_1 \leq P_{\max} \quad P_2 \leq P_{\max} \quad (4)$$

229 As consequence, the total power is limited to  $P=P_1+P_2 \leq 2P_{\max}$

230 In addition, for each pumping head, there is a minimum power threshold  $P_{\min}$  below which the  
231 group does not pump. This condition can be expressed as:

$$232 \quad \text{if } P_1 < P_{\min} \quad q(P_1) = 0 \quad \text{if } P_2 < P_{\min} \quad q(P_2) = 0 \quad (5)$$

233 The values of  $P_{\min}$  for each pumping head and of  $P_{\max}$  were obtained from the pumping tests.

234 The resulting flow rate propelled by the two pumps working in parallel  $Q(P)$  is:

$$235 \quad Q(P) = q(P_1) + q(P_2) = a_4 \cdot (P_1^4 + P_2^4) + a_3 \cdot (P_1^3 + P_2^3) + a_2 \cdot (P_1^2 + P_2^2) + a_1 \cdot (P_1 + P_2) + 2 \cdot a_0 \quad (6)$$

236 It is evident that for each value of  $P$  there will be a power distribution ratio which maximises  
237  $Q(P)$ .

238

### 239 *2.2.2. Distribution ratio $k$ of the available power $P$ between two pumps*

240 If  $k$  is defined as the distribution ratio of  $P$ , the power assigned to each pump will be:

$$241 \quad P_1 = k \cdot P \quad (0 \leq k \leq 0.5)$$

$$242 \quad P_2 = (1-k) \cdot P \quad (0.5 \leq (1-k) \leq 1)$$

243 This means that if there is an unequal distribution of power, pump 1 will work at a lower  
244 power and pump 2 will receive a higher power, i.e.  $P_1 \leq P_2$ .

245 Based on Equation (6), the resulting flow rate will be:

$$246 \quad Q(P) = a_4 \cdot [k^4 \cdot P^4 + (1-k)^4 \cdot P^4] + a_3 \cdot [k^3 \cdot P^3 + (1-k)^3 \cdot P^3] + a_2 \cdot [k^2 \cdot P^2 + (1-k)^2 \cdot P^2] + a_1 \cdot [k \cdot P + (1-k) \cdot P] + 2 \cdot a_0 \quad (7)$$

247 Due to the conditions established in Equations (4) and (5), a range of variation for  $k$  of  
248 between 0 and 0.5 is only possible for certain values of  $P$ . On this basis, two restrictions can  
249 be established:

250 (1) Since pump 2 receives higher power,  $P_2 = (1-k)P \leq P_{\max}$

251 (2) Since pump 1 receives lower power, if  $P_1 = k \cdot P < P_{\min}$ ,  $q(P_1) = 0$

252 These restrictions affect the power distribution strategy, since if the power assigned to pump  
253 1 is insufficient to produce flow rate, the total available power  $P$  must be assigned to pump 2,  
254 which implies  $k=0$  and  $1-k=1$ , provided that this does not violate restriction 1 (i.e.  $P_2 \leq P_{\max}$ ).

255 There will therefore be values of  $P$  for which the distribution ratio  $k$  will have a certain value,  
256 or will be limited to within a range of values. In view of this, the following cases can be  
257 considered:

258 (1)  $P < P_{\min}$ . Power is below the minimum threshold, and neither of the pumps are able to  
259 work, thus  $Q(P)=0$ . In accordance with restrictions 1 and 2, all power should be assigned to  
260 pump 2, but as it is lower than  $P_{\min}$ , it would constitute a loss and hence:  $k=0$ ,  $(1-k)=1$ ,  $P_1=0$ ,  
261  $P_2=P$ ,  $q(P_1)=q(P_2)=Q(P)=0$ .

262 (2)  $P_{\min} \leq P < 2P_{\min}$ . If the available power were distributed between the two pumps, pump 1  
263 would not reach the minimum power for pumping under any conditions, and the power  
264 assigned to it would be wasted. In order to avoid this, the total power must be assigned to  
265 pump 2 and therefore  $k=0$ ,  $(1-k)=1$ ,  $P_1=0$ ,  $P_2=P$ ,  $Q(P)=q(P_2)$ .

266 (3)  $2P_{\min} \leq P < P_{\max}$ . In theory,  $k$  can take values of between 0 and 0.5. However, if the power  
267 assigned to pump 1 is lower than  $P_{\min}$ , this does not generate flow rate, and therefore the  
268 total power must be assigned to pump 2. In other words, if  $P_1=k \cdot P < P_{\min}$ , which is equal to the  
269 condition  $k < (P_{\min}/P)$ , then  $k=0$ . Hence, the allowed values of  $k$  in this power range are  $k=0$   
270 and  $(P_{\min}/P) \leq k \leq 0.5$ .

271 (4)  $P_{\max} \leq P \leq 2P_{\max}$ . Pump 2 cannot receive the total available power, since restriction 1  
272 ( $P_2 \leq P_{\max}$ ) must be fulfilled. In other words,  $(1-k)P \leq P_{\max}$ , and  $k \geq 1 - (P_{\max}/P)$ .

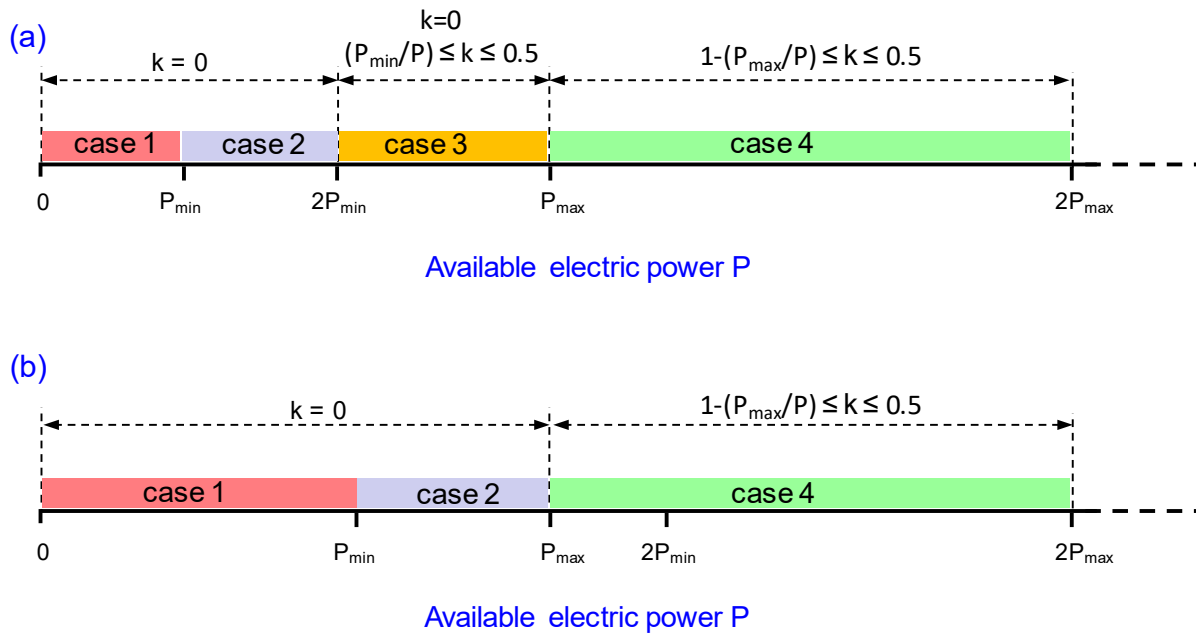
273 The distribution ratio  $k$  can therefore vary between  $1 - (P_{\max}/P) \leq k \leq 0.5$ .

274 The remaining available power may be lower than  $P_{\min}$ . In this case, it could not be  
275 assigned to pump 1 and it will therefore be a loss associated to PV pumping system design  
276 constraints since pump 2 cannot receive it.

277 (5)  $P > 2P_{\max}$ . The power supplied by the PV generator must be restricted to  $2P_{\max}$ . This power  
278 must be equally distributed between the two pumps ( $k=0.5$ ).

279 The five cases presented above apply whenever  $2P_{\min} < P_{\max}$ . If  $2P_{\min} \geq P_{\max}$ , these cases are all  
280 applicable except case 3 ( $2P_{\min} \leq P < P_{\max}$ ), which becomes meaningless. Moreover, for certain  
281 values of  $P$ , conditions 2 and 4 can be fulfilled simultaneously, meaning that  $P < 2P_{\min}$  and  
282  $P_{\max} \leq P \leq 2P_{\max}$ . In these circumstances,  $k$  should be that presented in case 4, since for safety  
283 purposes it is essential that  $P_2 = (1-k)P \leq P_{\max}$ .

284 Figure 3 summarises the possible  $k$ -values allowed versus the available electric power when  
285  $2P_{\min} < P_{\max}$  (Figure 3a) and when  $2P_{\min} \geq P_{\max}$  (Figure 3b).



286

287 *Figure 3. Possible values for the power distribution ratio  $k$  vs the available electric power when (a)  $2P_{\min} < P_{\max}$ ,*  
 288 *and (b)  $2P_{\min} \geq P_{\max}$ .*

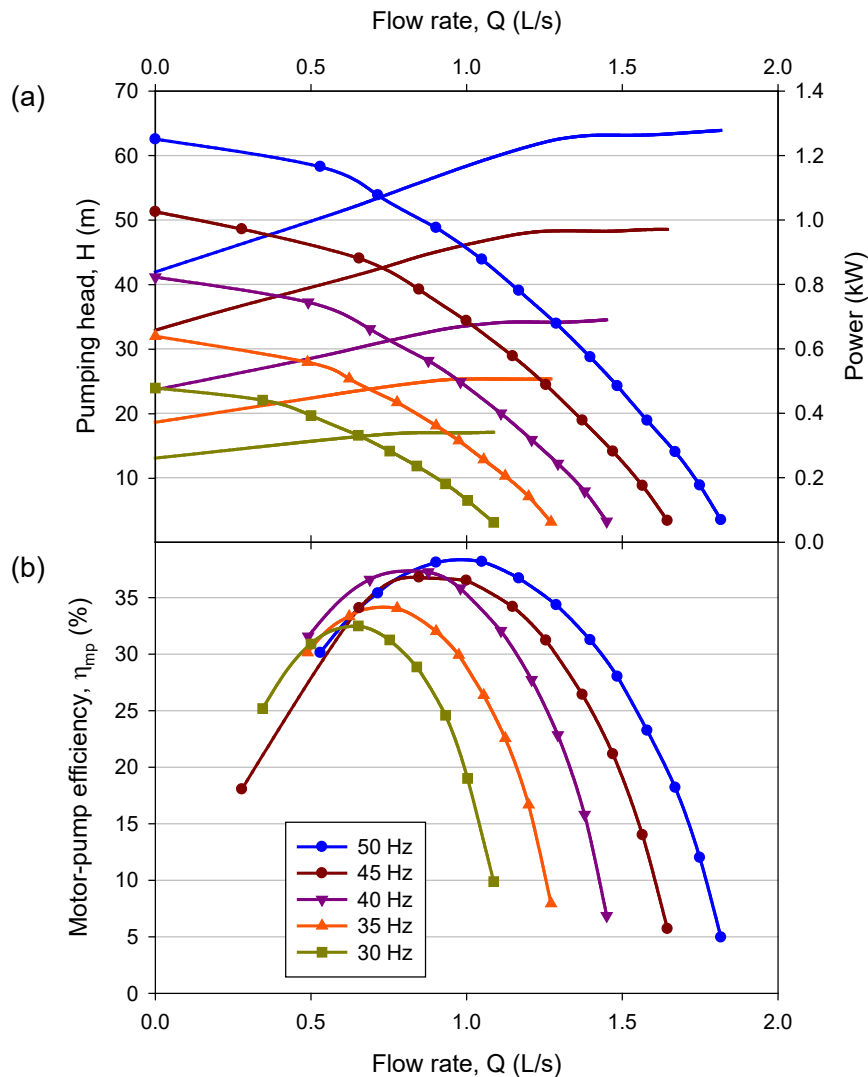
289 The value of the distribution ratio coefficient is  $k=0$  for available powers lower than  $2P_{\min}$  in  
 290 case  $2P_{\min} < P_{\max}$  (Figure 3a) or than  $P_{\max}$  in case  $P_{\max} < 2P_{\min}$  (Figure 3b). If the power is  
 291 higher than the lower of these two values,  $k$  varies within a certain range, as indicated in  
 292 Figure 3. Therefore, an optimal distribution ratio ( $k_{\text{opt}}$ ) that maximises the resulting flow rate  
 293 of the two pumps can be defined. Furthermore, the ranges of power over which  $k_{\text{opt}}$  can be  
 294 sought, are determined.

295

### 296 3. Pumping group tests

297 *3.1. Flow-head, flow-power and flow-efficiency curves of the motor-pump group at constant*  
 298 *frequency*

299 Figure 4a shows the Q-H and Q-P curves at frequencies of 50, 45, 40, 35 and 30 Hz for the  
 300 pumping group. Power refers to the electric power assigned to the motor-pump group.



301

302 *Figure 4. (a) Flow rate-head and flow rate-electric power curves, and (b) flow rate-efficiency curves of the*  
 303 *pumping group at various frequencies between 30 and 50 Hz.*

304 Figure 4a suggests that the operating range for the pump used here is approximately 10 to  
 305 60 m at a nominal frequency of 50 Hz. It can be observed that for very high pumping heads,  
 306 the possible margin for variation of the frequency is reduced; for example, at 50 m the  
 307 frequency can only be reduced to 45 Hz.

308 The efficiencies of the motor-pump group were calculated from the experimental results as  
 309 the ratio between the hydraulic power ( $P_h$ ) and the feeding electric power ( $P$ ).

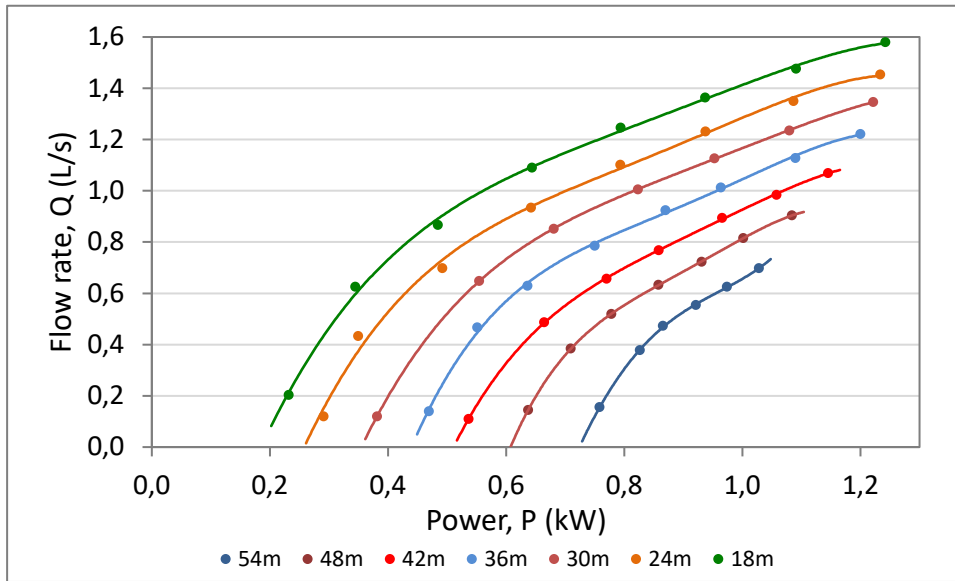
310 Figure 4b represents the  $Q$ - $\eta_{mp}$  curves at frequencies ranging from 30 to 50 Hz. The relation  
 311 between  $Q$  and  $H$  for higher efficiencies at each frequency can be observed. The highest  
 312 efficiency at a frequency of 50 Hz is 38.2 % with a flow rate of 1 L/s, while at 30 Hz, an  
 313 efficiency of 32.5 % with a flow rate of 0.7 L/s is achieved.

314

### 315 3.2. $Q$ - $P$ characteristic curve at constant head: Efficiency of the motor-pump group

316 Since  $H_{max}=60$  m, the heads used to obtain the  $Q$ - $P$  curves were 18, 24, 30, 36, 42, 48 and  
 317 54 m. The  $Q$ - $P$  curves were obtained with seven or eight experimental values for each  $H$

318 (Figure 5). Using those values, adjustment to the fourth-degree polynomial function in Eq. (2)  
 319 was carried out.



320  
 321 *Figure 5. Relation between the flow rate and the electric power of the pumping group at heads of 18, 24, 30, 36,*  
 322 *42, 48 and 54 m: experimental values and adjusted curves.*

323 The value of  $P_{max}$  can be obtained theoretically as  $P_{nominal}/\eta_{electric-motor}$  being in this case  
 324  $0.75/0.7 \approx 1.1$  kW. Nevertheless, it has been found experimentally (Figure 5) that  $P_{max}$  is  
 325 approximately 1.2 kW for all pumping tests.

326 For each value of H, there is a certain minimum operating power ( $P_{min}$ ), while the maximum  
 327 power allowed ( $P_{max}$ ) is around 1.2 kW in all cases (Table 1). It should be noted that  $P_{min}$   
 328 increases as the head increases.

329 *Table 1. Minimum operating power ( $P_{min}$ ) and maximum power allowed ( $P_{max}$ ) for the pumping group for each*  
 330 *pumping head tested*

H (m)	$P_{min}$ (kW)	$P_{max}$ (kW)
18	0.20	1.20
24	0.26	
30	0.36	
36	0.45	
42	0.52	
48	0.61	
54	0.73	

331  
 332 Table 2 summarises the results of the regression adjustments of the Q-P curves and the  
 333 corresponding regression coefficients ( $r^2$ ) obtained for the heads tested.

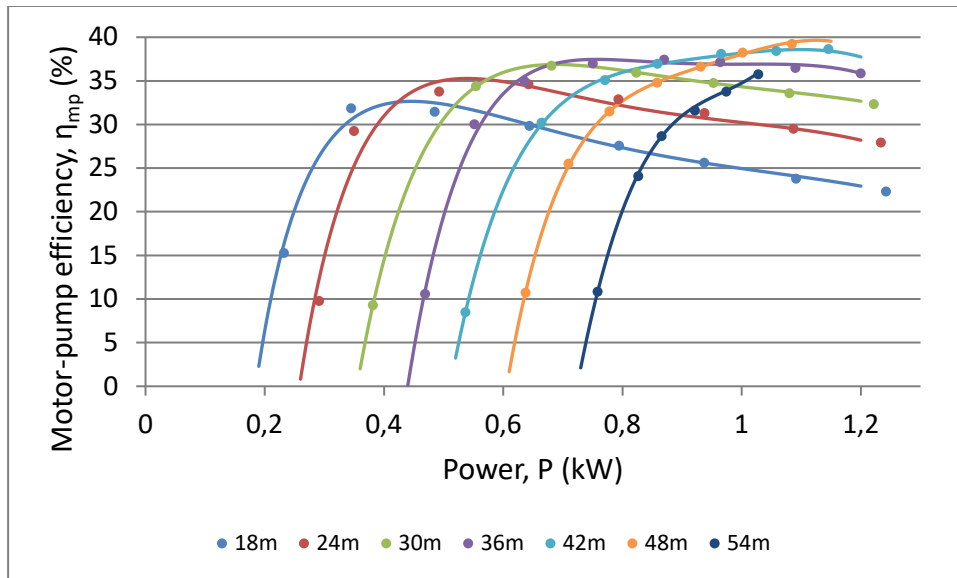
334 *Table 2. Adjusted equations  $q(P)$  and regression coefficients ( $r^2$ ) for the pumping group for each head tested*

H (m)	REGRESSION EQUATION $q(P)=a_4 \cdot P^4+a_3 \cdot P^3+a_2 \cdot P^2+a_1 \cdot P+a_0$	$r^2$
18	$q=-3.051 \cdot P_{mp}^4+10.737 \cdot P_{mp}^3-14.147 \cdot P_{mp}^2+9.146 \cdot P_{mp}-1.2721$	0.99871
24	$q=-4.582 \cdot P_{mp}^4+15.942 \cdot P_{mp}^3-20.625 \cdot P_{mp}^2+12.709 \cdot P_{mp}-2.1603$	0.99604
30	$q=-4.290 \cdot P_{mp}^4+16.530 \cdot P_{mp}^3-23.886 \cdot P_{mp}^2+16.236 \cdot P_{mp}-3.4240$	0.99999
36	$q=-10.340 \cdot P_{mp}^4+38.341 \cdot P_{mp}^3-52.882 \cdot P_{mp}^2+33.152 \cdot P_{mp}-7.2259$	0.99900

42	$q=-10.605 \cdot P_{mp}^4+40.013 \cdot P_{mp}^3-56.678 \cdot P_{mp}^2+36.835 \cdot P_{mp}-8.6385$	0.99989
48	$q=-23.530 \cdot P_{mp}^4+89.984 \cdot P_{mp}^3-128.820 \cdot P_{mp}^2+83.039 \cdot P_{mp}-19.865$	0.99999
54	$q=23.563 \cdot P_{mp}^4-60.966 \cdot P_{mp}^3+45.190 \cdot P_{mp}^2-0.386 \cdot P_{mp}-6.746$	0.99980

335

336 From the experimental values for Q and P and from the adjusted curves,  $\eta_{mp}$  was determined  
 337 for each H (Figure 6).



338

339 *Figure 6. Relation between the efficiency and the power of the pumping group at heads of 18, 24, 30, 36, 42, 48*  
 340 *and 54 m: experimental values and adjusted curves.*

341

342 In general, it is observed for all heads that the efficiencies increase rapidly with power,  
 343 reaching a maximum after which a moderate decrease is seen. The maximum efficiencies  
 344 achieved for heads of 48 and 18 m are 39.6 % and 32.6 %, respectively. At 54 m the  
 345 pumping group works at low efficiencies at almost all power rates. Thus, this head is not  
 346 considered in this study.

347

#### 348 4. Results and Discussion

##### 349 4.1. Optimal power distribution ratio between the two pumps

350 Since  $P_{min}$  and  $P_{max}$  are determined, it can be established at each pumping head whether  
 351  $2P_{min} < P_{max}$  or  $2P_{min} \geq P_{max}$ . As shown in Section 2.2.2, the intervals of variation of k (Figure 3)  
 352 and the ranges of power over which  $k_{opt}$  should be sought can be specified in each case.  
 353 These results are summarised in Table 3. Two possible cases are presented since for heads  
 354 of 18, 24, 30, 36 and 42 m it is  $2P_{min} < P_{max}$ , while at H=48 m it is  $2P_{min} \geq P_{max}$ .

355

356 *Table 3. Relationship between the values  $P_{min}$  and  $P_{max}$ , intervals of variation of the power distribution coefficient*  
 357 *k, and ranges of power in which  $k_{opt}$  (the value of k that maximises the resulting flow rate of the two pumps)*  
 358 *should be sought, at each of the tested pumping heads.*

H(m)	$2P_{min}$ (kW)	$P_{max}$ (kW)	Relationship $2P_{min} \leftrightarrow P_{max}$	Intervals of variation of k	Ranges of power P for $k_{opt}$
18	0.4	1.2	$2P_{min} < P_{max}$	k=0 and $(P_{min}/P) \leq k \leq 0.5$	$2P_{min} \leq P \leq P_{max}$
24	0.52	1.2			
30	0.72	1.2			
36	0.9	1.2			
42	1.04	1.2	$2P_{min} \geq P_{max}$	$1 - (P_{max}/P) \leq k \leq 0.5$	$P_{max} < P \leq 2P_{max}$
48	1.22	1.2			

359

360 The values of the coefficients  $a_0$ ,  $a_1$ ,  $a_2$ ,  $a_3$  and  $a_4$  obtained from the adjustment by regression  
 361 of the function  $q(P)$  (Table 2) allow applying Eq. (7) to determine the flow rate pumped by the  
 362 two pumps, based on the value of k at each pumping head and the available power.

363 Next, the implementation of the distribution strategy set out in the Materials and Methods  
 364 section is described in more detail for each case at the specific pumping heads.

365 **4.1.1. Pumping when  $2P_{min} < P_{max}$**

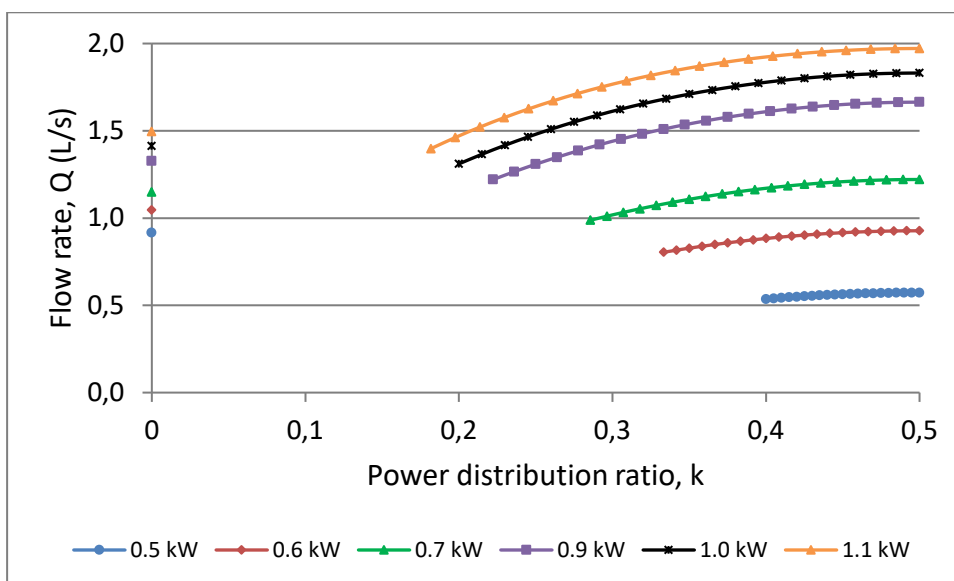
366 Considering H=18 m as an example, when  $P < 2P_{min}$ ,  $k=0$  (Figure 3a), and the intervals of  
 367 power in which the value of  $k_{opt}$  should be found are:  $2P_{min} \leq P \leq P_{max}$  and  $P_{max} < P \leq 2P_{max}$  (Table  
 368 3).

369 (1) Power in the range  $2P_{min} \leq P \leq P_{max}$  (i.e.  $0.40 \text{ kW} \leq P \leq 1.2 \text{ kW}$ )

370 The values of the power distribution ratio are either  $k=0$  or any value within the interval  
 371  $(P_{min}/P) \leq k \leq 0.5$ .

372 Figure 7 shows the flow rate resulting from the two pumps  $Q(P)$  based on k and for six  
 373 values of available power within the range considered. The table attached to the figure gives  
 374 the value of  $k_{opt}$  and the maximum resulting flow rate ( $Q_{max}$ ) at each power.

375



376

P (kW)	0.5	0.6	0.7	0.9	1.0	1.1

$(P_{min}/P)$	0.400	0.333	0.286	0.222	0.200	0.182
$k_{opt}$	0.00	0.00	0.50	0.50	0.50	0.50
$Q_{max}$ (L/s)	0.92	1.05	1.22	1.66	1.83	1.97

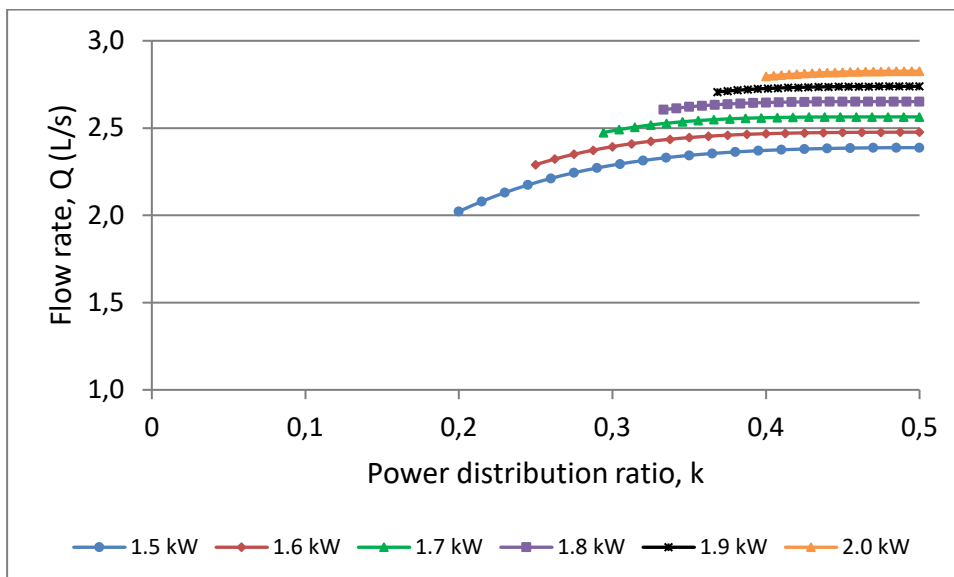
377 Figure 7. Flow rate resulting from the two pumps  $Q(P)$  at  $H=18$  m vs power distribution ratio  $k$ , for six values of  
378 available power (0.5, 0.6, 0.7, 0.9, 1.0 and 1.1 kW) within the range  $2P_{min} \leq P \leq P_{max}$ . Only the flow rates for the  
379 accepted values of  $k$ :  $k=0$  and  $(P_{min}/P) \leq k \leq 0.5$  are shown. The attached table gives the values of  $k_{opt}$  and the  
380 corresponding maximum flow rates for each available power.

381  
382 Within this range of values for the power,  $k_{opt}$  only takes the values 0 and 0.5. Furthermore,  
383 there is a value of the power defined as  $P_e$  (between 0.6 and 0.7 kW) below which  $k_{opt}=0$ ,  
384 and above which  $k_{opt}=0.5$ . This value  $P_e$  therefore represents the power above which the two  
385 pumps should work in parallel with a power distribution at 50%. The expression for its  
386 calculation is given below.

387 (2) Power in the range  $P_{max} < P \leq 2P_{max}$  (i.e. 1.2 kW  $< P \leq 2.4$  kW)

388 The parameter  $k$  can take any value in the interval  $1-(P_{max}/P) \leq k \leq 0.5$  (in this case,  $1-$   
389  $(1.2/P) \leq k \leq 0.5$ ), where  $1-(P_{max}/P)$  denotes the minimum value of  $k$ ,  $k_{min}$ , for all  $P$  in this  
390 interval.

391 Figure 8 shows the flow rate  $Q(P)$  in accordance with  $k$ , for six values of available power in  
392 the range 1.2 kW  $< P \leq 2.4$  kW. The table attached to the figure gives the value of  $k_{opt}$  and the  
393 corresponding  $Q_{max}$  for each power.



394

P (kW)	1.5	1.6	1.7	1.8	1.9	2.0
$k_{min}=1-(P_{max}/P)$	0.200	0.250	0.294	0.333	0.368	0.400
$k_{opt}$	0.50	0.50	0.479	0.475	0.50	0.50
$Q_{max}$ (L/s)	2.3879	2.4765	2.5640	2.6516	2.7391	2.8260
Q for $k=0.5$ (L/s)			2.5640	2.6515		

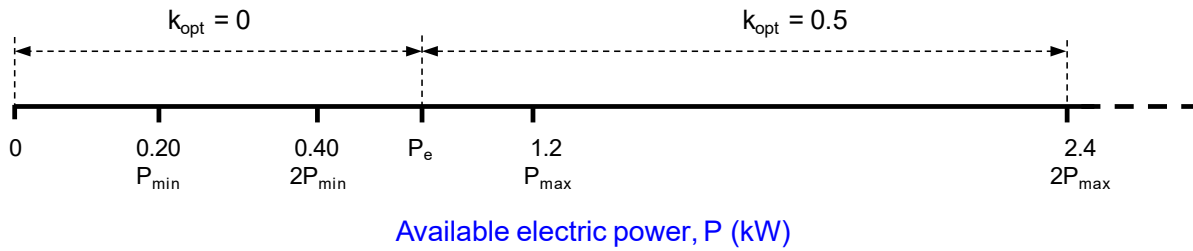
395 Figure 8. Flow rate resulting from the two pumps  $Q(P)$  at  $H=18$  m vs power distribution ratio  $k$ , for six values of  
396 available power: 1.5, 1.6, 1.7, 1.8, 1.9 and 2.0 kW, within the range  $P_{max} < P \leq 2P_{max}$ . The attached table gives the



397 value of  $k_{opt}$  and the corresponding maximum flow rate for each power. In the cases where  $k_{opt} < 0.5$ , the flow rate  
 398 obtained at  $k=0.5$  is also given.  
 399

400 It is observed that  $k_{opt}=0.5$  for most of the P values analysed here; in cases where  $k_{opt}$  is not  
 401 equal to 0.5 (i.e. at  $P=1.7$  kW and  $1.8$  kW), it takes values close to 0.5 and  $Q_{max}$  is practically  
 402 the same as that obtained for  $k=0.5$ . It can therefore be considered that  $k_{opt}=0.5$  for all P  
 403 within the studied interval.

404 Figure 9 summarises the results for  $H=18$  m.



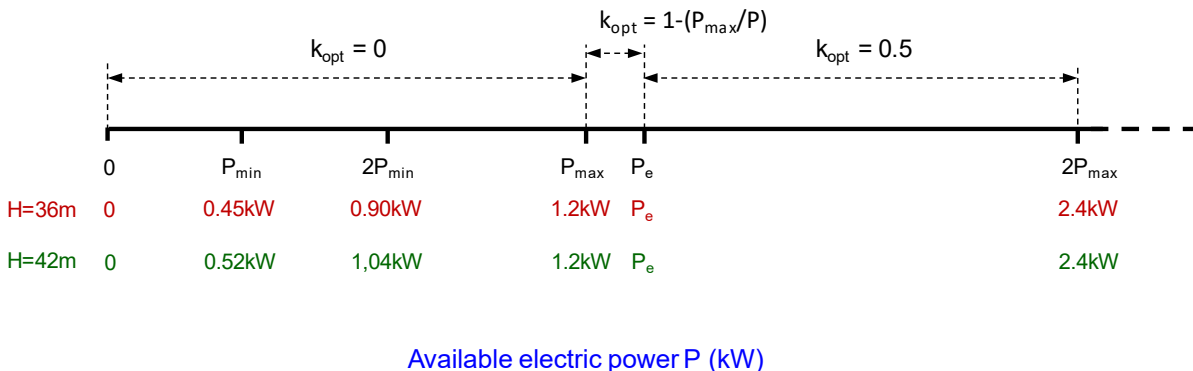
405

406 *Figure 9. Values of the optimal power distribution ratio  $k_{opt}$  vs available electric power, for a pumping head  $H=18$   
 407 m. The value of  $P_e$  is between 0.6 and 0.7 kW.*

408 Pumping heads of 24, 30 36 and 42 m give the same behaviour as  $H=18$  m, since  $2P_{min} < P_{max}$   
 409 (Table 3).

410 The cases  $H=24$  m and  $H=30$  m (results not shown) differ from the case  $H=18$  m only in  
 411 terms of the value of  $P_e$ , which is between 0.8 and 0.9 kW ( $H=24$  m), and between 1.05 and  
 412 1.1 kW ( $H=30$  m). Note that in all three cases (18, 24 and 30 m)  $P_e < P_{max}$ .

413 However, for both  $H=36$  m and  $H=42$  m (results not presented), it is verified that  $P_e > P_{max}$ .  
 414 This means that in the interval of power between  $P_{max}$  and  $P_e$ , a value of  $k=0$  would mean  
 415 that the power assigned to the pump 2 would be higher than  $P_{max}$ . Hence,  $k_{opt}=1-(P_{max}/P)$ ,  
 416 meaning that  $P(1-k)=P_{max}$ . The remaining available power only could be assigned to pump 1  
 417 if it is higher than  $P_{min}$ . Otherwise it would be a lost. Figure 10 illustrates the conclusions in  
 418 these cases ( $H=36$  m and  $H=42$  m). It is found that the value of  $P_e$  is between 1.23 and 1.3  
 419 kW for  $H=36$  m, whereas for  $H=42$  m is between 1.3 and 1.4 kW.



420

421 *Figure 10. Values of optimal power distribution ratio  $k_{opt}$  vs available electric power, for pumping heads  $H=36$  m  
 422 ( $P_e$  between 1.23 and 1.3 kW) and  $H=42$  m ( $P_e$  between 1.3 and 1.4 kW).*

423

424 **4.1.2. Pumping when  $2P_{min} \geq P_{max}$**

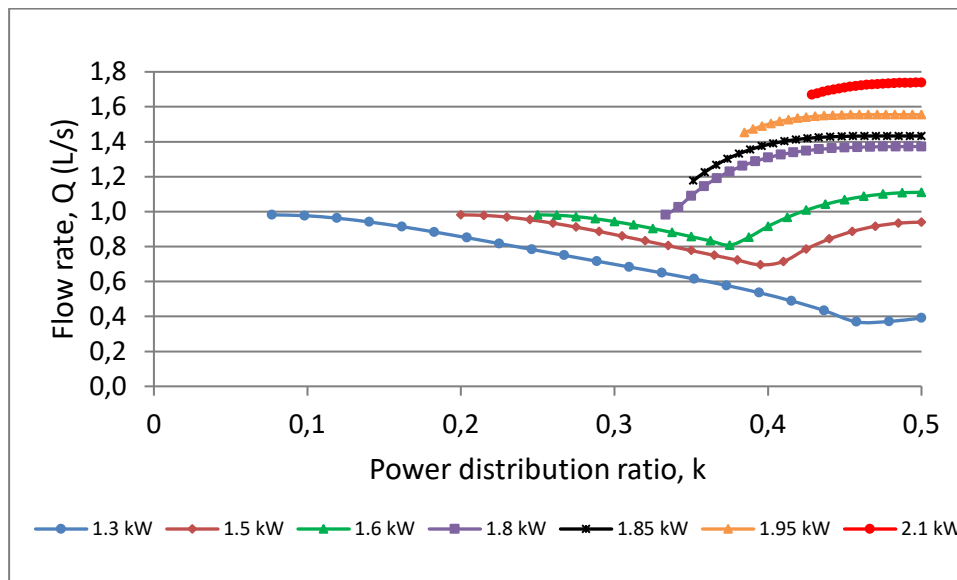
425 It should be noted that the condition  $2P_{\min} < P_{\max}$  occurs under the normal operating conditions  
 426 of the motor-pump groups. The case  $2P_{\min} \geq P_{\max}$  occurs only for high pumping heads within  
 427 the application range of the selected pump (e.g. the case of a pumping system in which there  
 428 is a significant decrease in the water table; the pump is selected so that these are not the  
 429 normal operating conditions). In the present study the condition  $2P_{\min} \geq P_{\max}$  only occurs for  
 430 the highest pumping head,  $H=48$  m.

431 Considering then  $H=48$  m as an example of this case, the range of powers in which in which  
 432  $k_{\text{opt}}$  should be sought is  $P_{\max} < P \leq 2P_{\max}$  (Table 3). For  $P \leq P_{\max}$  (i.e.  $P \leq 1.2$  kW),  $k_{\text{opt}}=0$  and all the  
 433 power is assigned to pump 2 (Figure 3b).

434 If power is in the range  $P_{\max} < P \leq 2P_{\max}$  (i.e.  $1.2 \text{ kW} < P \leq 2.4 \text{ kW}$ ),  $k$  can take any value within  
 435 the interval  $1 - (1.2/P) \leq k \leq 0.5$ .

436 Figure 11 presents the resulting flow rate  $Q(P)$  vs  $k$ , for seven values of available power  
 437 within the range  $1.2 \text{ kW} < P \leq 2.4 \text{ kW}$ . The attached table shows the values of  $k_{\min}$ ,  $k_{\text{opt}}$ , and  
 438  $Q_{\max}$  at each considered power.

439



440

P (kW)	1.3	1.5	1.6	1.8	1.85	1.95	2.1
$k_{\min}=1-(P_{\max}/P)$	0.077	0.200	0.250	0.333	0.351	0.385	0.429
$k_{\text{opt}}$	0.077	0.200	0.500	0.500	0.478	0.471	0.500
$Q_{\max}$ (L/s)	0.9815	0.9815	1.1106	1.3724	1.4330	1.5551	1.7375
Q for $k=0.5$ (L/s)					1.4328	1.5545	

441 *Figure 11. Flow rate resulting from the two pumps  $Q(P)$  at  $H=48$  m vs power distribution ratio  $k$ , for seven values  
 442 of available power: 1.3, 1.5, 1.6, 1.8, 1.85, 1.95 and 2.1 kW, within the range  $P_{\max} \leq P \leq 2P_{\max}$ . The attached table  
 443 gives the values of  $k_{\text{opt}}$  and the corresponding maximum flow rate for each value of available power.*

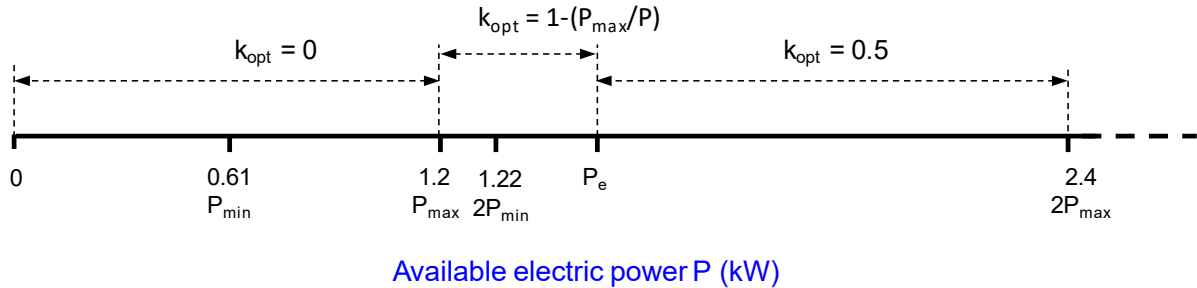
444

445 It should be noted that there is a value of power  $P_e$  (between 1.5 and 1.6 kW) below which  
 446  $k_{\text{opt}}=k_{\min}$ . For  $P \geq P_e$ , the  $Q_{\max}$  occurs when  $k=0.5$ , except when  $P$  is around 1.85-1.95 kW. In  
 447 these cases,  $k_{\text{opt}}$  is slightly less than 0.5 although the resulting  $Q_{\max}$  is practically the same as  
 448 that obtained at a distribution ratio  $k=0.5$ .

449 In fact, for  $P < P_e$ , it should be  $k_{opt} = 0$ , but this would mean that the power assigned to pump 2  
 450 would be  $P(1-k) > P_{max}$ . Thus,  $k_{opt} = 1 - (P_{max}/P)$ , meaning that  $P(1-k) = P_{max}$ . It is possible that the  
 451 power assigned to pump 1 may be insufficient for pumping.

452 Therefore, over the whole interval of powers ( $1.2 \text{ kW} < P \leq 2.4 \text{ kW}$ ),  $k_{opt} = 1 - (P_{max}/P)$  when  $P < P_e$   
 453 and  $k_{opt} = 0.5$  when  $P > P_e$ .

454 Figure 12 illustrates the results of this case ( $H=48 \text{ m}$ ).



455

456 *Figure 12. Values of optimal power distribution ratio  $k_{opt}$  vs available electric power, for pumping head  $H=48 \text{ m}$ .  $P_e$   
 457 is a value between  $1.5$  and  $1.6 \text{ kW}$ .*

458 Note that at heads of  $36$ ,  $42$ , and  $48 \text{ m}$ , the condition  $P_e > P_{max}$  is fulfilled and the same  
 459 conclusions can be drawn for the calculation of  $k_{opt}$  (Figures 10 and 12).

460 There is therefore no power distribution ratio other than  $0$  and  $0.5$  which maximises the flow  
 461 rate, except that indicated to limit the power assigned to one of the pumps up to  $P_{max}$ .

462 These experimental tests were also carried out for  $1.5 \text{ kW}$  pumps, with similar results (not  
 463 reported here), and this confirms the applicability of these conclusions to pumps of different  
 464 powers.

465

#### 466 4.2. Power $P_e$ and determination of its value

467 This section explains how the value of  $P_e$  is determined.

468 In all cases, it is found that when  $P > P_e$ , the two pumps must work at a power distribution of  
 469  $50 \%$  ( $k_{opt} = 0.5$ ).

470 The flow rate propelled by both pumps in parallel, each of which receives half of the available  
 471 power ( $k=0.5$ ), is:

$$472 \quad Q(P) = q(P/2) + q(P/2) = 2 \cdot q(P/2) = 2 \cdot [a_4 \cdot (P/2)^4 + a_3 \cdot (P/2)^3 + a_2 \cdot (P/2)^2 + a_1 \cdot P/2 + a_0] \quad (8)$$

473 The flow rate from a single pump can be compared with that from two pumps in parallel with  
 474  $k=0.5$ . Figure 13 shows the curves for the flow rate-power of a single pump  $q(P)$  and for two  
 475 pumps in parallel  $Q(P)$  with a power distribution of  $50 \%$  ( $k=0.5$ ). Two cases can be  
 476 considered:

477 (a) The curves  $Q(P)$  and  $q(p)$  intersect at a value of power  $P < P_{max}$  (Figure 13a).

478 It should be noted that for values of power higher than the intersection point, the flow rate for  
 479 two pumps in parallel with  $k=0.5$  is higher than that for a single pump fed with all the  
 480 available power. Thus, if  $P > P_e$ , then  $Q(P) > q(P)$ . The power at the intersection point is

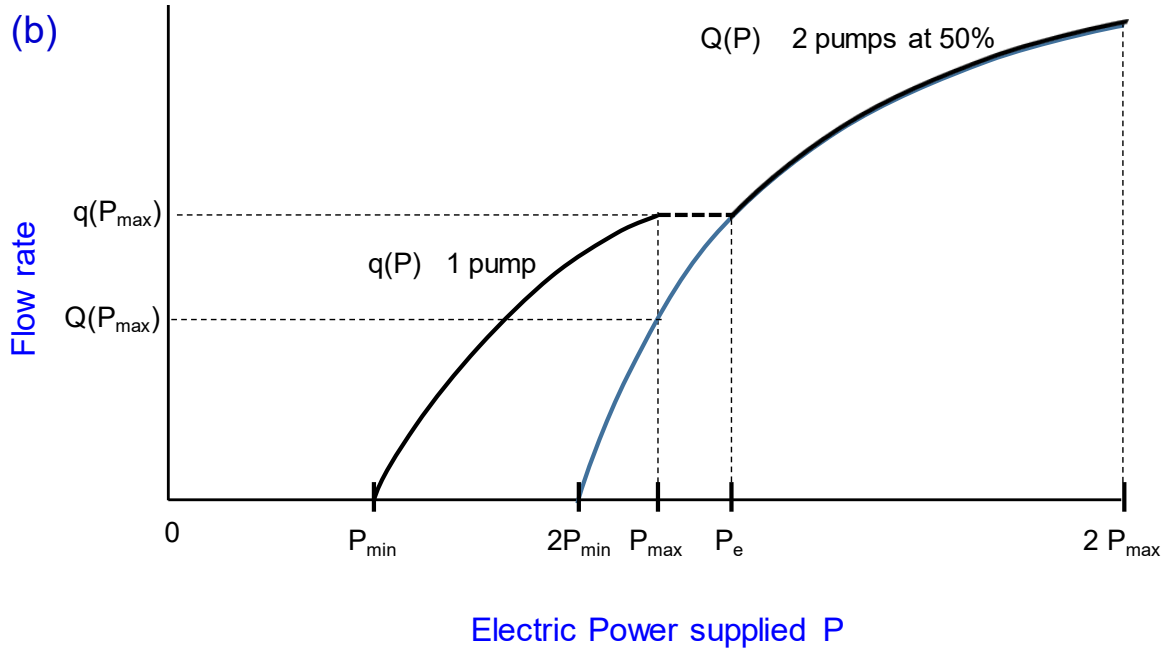
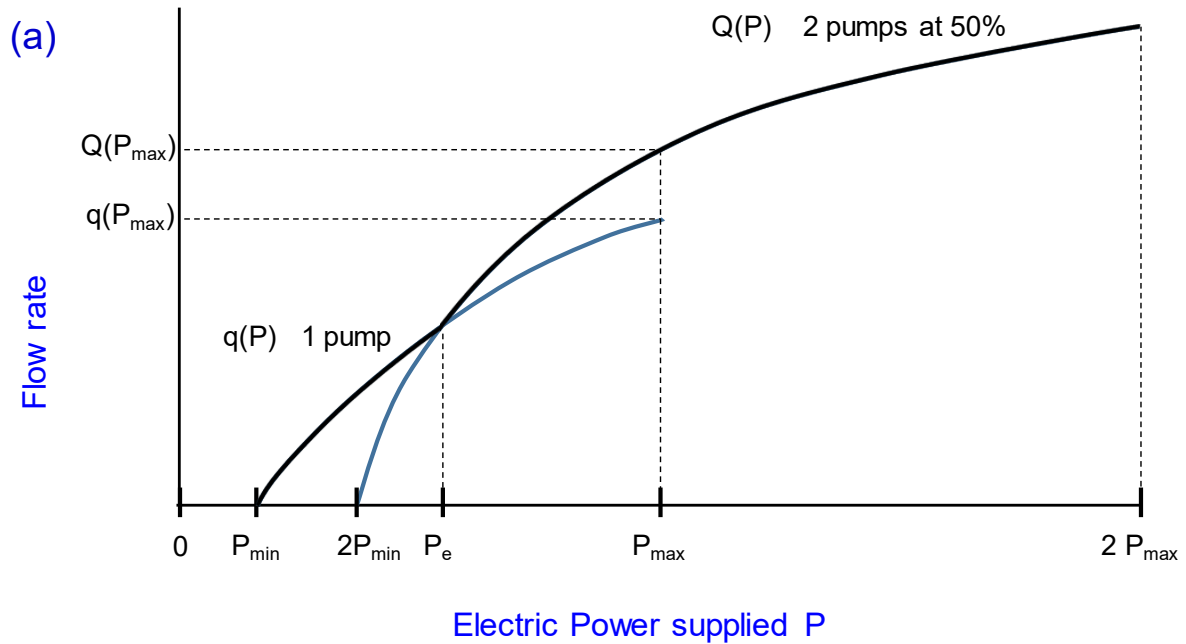
481 precisely the value of  $P_e$  for heads of 18, 24 and 30 m, all of which have a similar power  
482 distribution.

483 (b) The curves  $Q(P)$  and  $q(p)$  do not intersect for values of power  $P < P_{max}$  (Figure 13b).

484 In this case, when  $P < P_{max}$ , the flow rate for a single pump  $q(P)$  is higher than that for two  
485 pumps  $Q(P)$  with  $k=0.5$ . However, even if the value of  $P_{max}$  is exceeded, only a single pump  
486 can work, although it cannot be fed with all the available power. The maximum power  
487 assigned to this pump must be kept equal to  $P_{max}$ , and the excess cannot be assigned to the  
488 other pump, (given that this may be insufficient for pumping). Then it would be a loss if it  
489 could not be allocated for other uses. This is equivalent to a power distribution ratio of  $k=1-$   
490  $(P_{max}/P)$ .

491 When the available power exceeds a certain value, it is verified that  $Q(P) > q(P)$ , meaning that  
492 the two pumps must work in parallel with  $k=0.5$ . This value corresponds to the value of  $P_e$   
493 obtained for pumping at heads of 36, 42 and 48 m, in which, as stated above, the power  
494 distribution is similar.

495 In order to establish an adequate working strategy and the values of  $k_{opt}$  for each  $H$ , it is  
496 required to determine which case applies, i.e. (a) or (b) (Figure 13), and to obtain the value of  
497  $P_e$ .



498

499 *Figure 13. Flow rate-power curves for a single pump ( $q(P)$ ) and for two pumps in parallel with a power distribution*  
 500 *ratio of 50 % ( $Q(P)$ ), for (a)  $P_e < P_{max}$ ; (b)  $P_e > P_{max}$ .*

501 In order to determine whether pumping at a certain head corresponds to case (a) or (b), as  
 502 shown in Figure 13, the flow rates  $q(p)$  and  $Q(P)$  at  $P=P_{max}$  are compared. Thus, if  
 503  $q(P_{max}) < Q(P_{max})$  it is case (a), while if  $q(P_{max}) > Q(P_{max})$  it is case (b). In practice, it is simple to  
 504 verify this fact at any facility. Since  $Q(P_{max}) = 2q(P_{max}/2)$ , it is sufficient to perform a pumping  
 505 test with a single pump and to check whether  $q(P_{max})$  is lower (case (a)), or higher (case (b)),  
 506 than  $2q(P_{max}/2)$ .

507 In case (a),  $P_e < P_{max}$  and the value of  $P_e$  is obtained by equating Equations (2) and (8), giving:

508  $(7/8) \cdot a_4 \cdot P^4 + (3/4) \cdot a_3 \cdot P^3 + (1/2) \cdot a_2 \cdot P^2 - a_0 = 0$  (9)

509 To solve Equation (9) and obtain the value of  $P_e$ , numerical methods can be used. The  
 510 optimal distribution strategy for the available power is as follows: if  $P \leq P_e$ , all the power must  
 511 be assigned to one of the pumps ( $k=0$ ), and if  $P > P_e$ , the power must be distributed at 50 %  
 512 between the two pumps ( $k=0.5$ ).

513 In case (b),  $P_e > P_{max}$ , and the value of  $P_e$  above which both pumps function can be obtained  
 514 from the solution of the equation:

515  $Q(P) = q(P_{max})$

516  $q(P_{max})$  is expressed as:

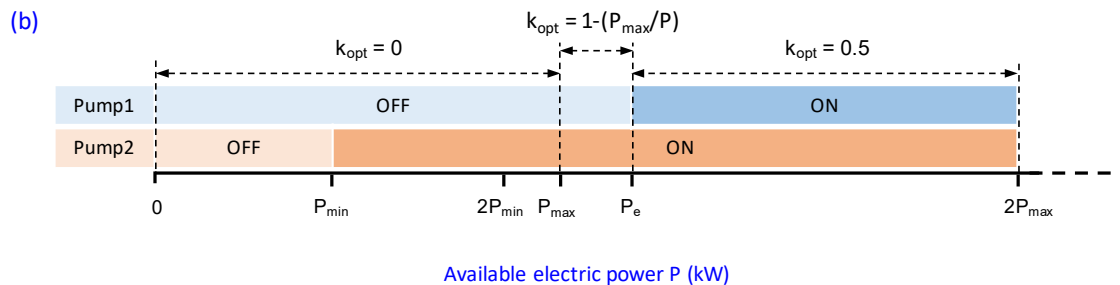
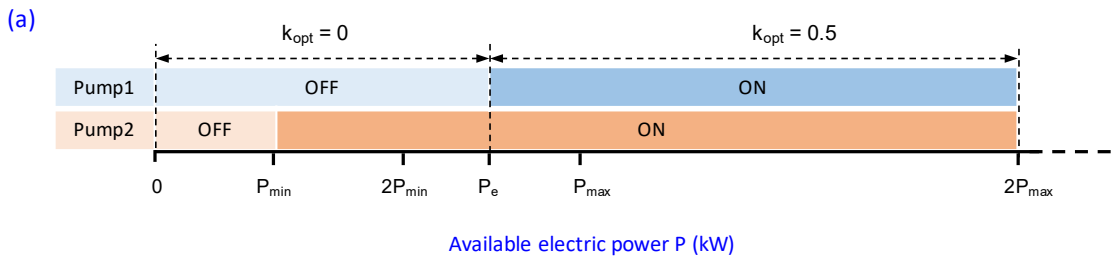
517  $q(P_{max}) = a_4 \cdot P_{max}^4 + a_3 \cdot P_{max}^3 + a_2 \cdot P_{max}^2 + a_1 \cdot P_{max} + a_0$  (10)

518 Equating Equations (8) and (10) gives:

519  $(a_4/8) \cdot P^4 + (a_3/4) \cdot P^3 + (a_2/2) \cdot P^2 + a_1 \cdot P + 2 \cdot a_0 = q(P_{max})$  (11)

520 The solution to the above equation leads to obtain the value of  $P_e$ . In this case, the optimal  
 521 distribution strategy for the available power is as follows: when  $P \leq P_{max}$ , all the power must be  
 522 assigned to one of the pumps (pump 2), and  $k=0$ . When  $P$  is in the range  $P_{max} < P \leq P_e$ , pump 2  
 523 must operate with  $P_{max}$  and the excess power is transferred to pump 1, ( $k=1-(P_{max}/P)$ ), only in  
 524 case that the power received ( $P-P_{max}$ ) is higher than  $P_{min}$ . Finally, if  $P > P_e$ , the power must be  
 525 distributed at 50 % between the two pumps ( $k=0.5$ ).

526 Figure 14 shows the optimal distribution strategy ( $k_{opt}$ ) vs  $P$  in cases (a) ( $P_e < P_{max}$ ) and (b)  
 527 ( $P_e > P_{max}$ ). The different operating modes in each case (ON/OFF status of each pump) have  
 528 also been included.



529

530 *Figure 14. Optimal distribution strategy for the available power for (a)  $P_e < P_{max}$ ; (b)  $P_e > P_{max}$ . Operating mode*  
 531 *(ON/OFF status) of both pumps in each case.*

532

533 Table 4 gives the ranges in which the value of  $P_e$  is found for each H (previously obtained)  
 534 and its relationship with  $P_{max}$ . It should be noted that the power distribution strategy for the  
 535 lower pumping heads (18, 24 and 30 m) corresponds to case (a) with  $P_e < P_{max}$ , while that for  
 536 the higher pumping heads (36, 42 and 48 m) corresponds to case (b) with  $P_e > P_{max}$ .

537

538 *Table 4. Range of values of P for which the value of  $P_e$  is found and relationship between  $P_e$  and  $P_{max}$  for all*  
 539 *pumping heads*

H(m)	$P_e$ Rank (kW)	$P_{max}$ (kW)	Relationship $P_e \leftrightarrow P_{max}$
18	0.6-0.7	1.2	$P_e < P_{max}$
24	0.8-0.9		
30	1.05-1.1		
36	1.23-1.3	1.2	$P_e > P_{max}$
42	1.3-1.4		
48	1.5-1.6		

540

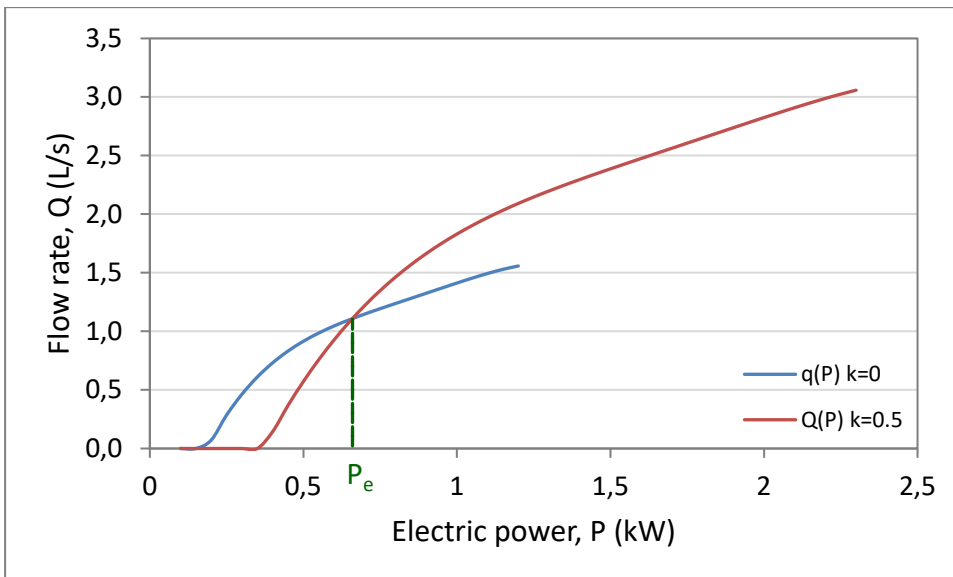
541 Based on the previous considerations, the value of  $P_e$  is determined below for the different  
 542 pumping heads. The conclusion drawn here can be used to define the strategy for pumping  
 543 heads  $H=18$  m and  $H=42$  m, as representative examples of the two possible cases (Table 4).

544  *$P_e$  and power distribution strategy at  $H=18$  m*

545 Firstly, the values of  $q(P_{max})$  and  $Q(P_{max})=2 \cdot q(P_{max}/2)$  are compared. Substituting the  
 546 corresponding values, since  $q(P_{max}) < Q(P_{max})$ , it is case (a), i.e.  $P_e < P_{max}$ . By substituting and  
 547 solving Equation (9), the value of  $P_e$  is determined (table 5).

548 Figure 15 shows the optimal distribution strategy for the available power at  $H=18$  m.

549



550

551 *Figure 15. Flow rate-power curves for a single pump of 0.75 kW ( $k=0$ ), and for two pumps of 0.75 kW working in*  
 552 *parallel with ratio of power distribution of 50 % ( $k=0.5$ ), pumping at  $H=18$  m.  $P_e = 0.660$  kW.*

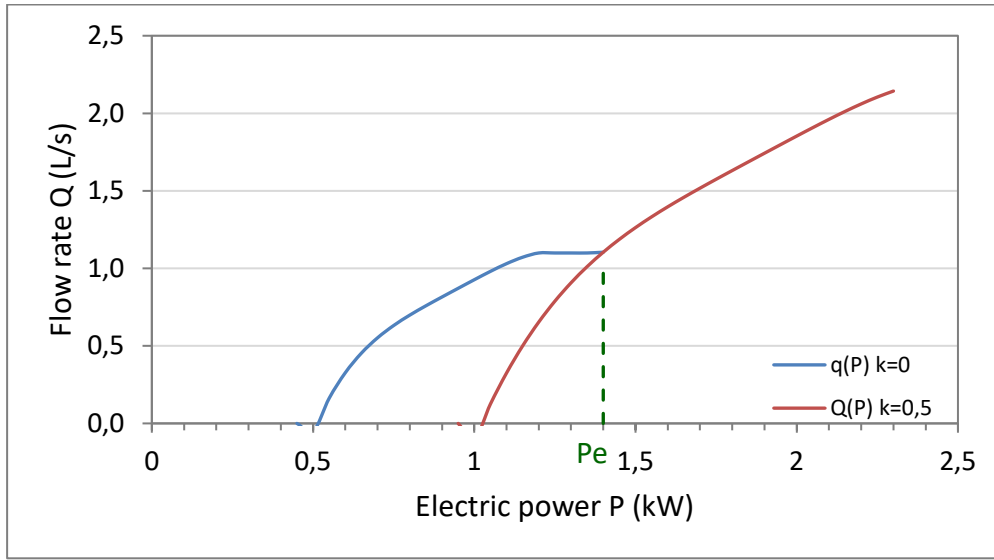
553

554  $P_e$  and power distribution strategy at  $H=42$  m

555 As in the case of  $H=18$  m, the values for  $q(P_{max})$  and  $Q(P_{max})=2 \cdot q(P_{max}/2)$  are first compared.  
556 Since  $q(P_{max}) > Q(P_{max})$ , it is case (b), i.e.  $P_e > P_{max}$ . By substituting and solving Equation (11),  
557 the value for the power  $P_e$  can be obtained (Table 5).

558 Figure 16 shows the optimal available power distribution strategy at  $H=42$  m.

559



560

561 *Figure 16. Flow rate-power curves for a single pump 0.75 kW ( $k=0$ ), and for two pumps of 0.75 kW in parallel with*  
562 *power distribution at 50 % ( $k=0.5$ ), pumping at  $H=42$  m.  $P_e = 1.40$  kW.*

563

564 Table 5 summarises the results of determining  $P_e$  for all pumping heads tested in this work,  
565 and shows that the calculated value for  $P_e$  is within the previously estimated range.

566 *Table 5. Calculated  $P_e$  values for all pumping heads tested*

H(m)	$q(P_{max})$ (L/s)	$Q(P_{max})$ (L/s)	case	$P_e$ (kW)
18	1.558	2.092	(a) $P_e < P_{max}$	0.660
24	1.437	1.78		0.824
30	1.332	1.466		1.083
36	1.219	1.139	(b) $P_e > P_{max}$	1.243
42	1.099	0.654		1.400
48	0.982	0.000		1.522

567

## 568 5. Conclusions

569 In this paper, a method of distributing the power generated in a photovoltaic pumping system  
570 equipped with two equal 0.75 kW pumps working in parallel is investigated.



571 The pumps were experimentally characterised by the determination of the Q-H and Q-P  
572 curves at five different working frequencies (30-50 Hz), and at six pumping heads (18-48 m).

573 A strategy for the distribution of the generated power is established which maximises the flow  
574 rate pumped by the set of both pumps. For this purpose, a distribution ratio of the available  
575 power between the two pumps,  $k$ , is defined.

576 The possible values that  $k$  can take are analysed based on the available power  $P$ . These can  
577 be grouped into two cases, depending on whether  $2P_{\min} < P_{\max}$  or  $2P_{\min} \geq P_{\max}$ , where  $P_{\min}$  is the  
578 minimum power required to start the pumping at a certain head, and  $P_{\max}$  is the maximum  
579 power allowed for the pumping group.

580 An optimal distribution ratio ( $k_{\text{opt}}$ ) of the power between the two pumps can be defined. The  
581 power ranges in which  $k_{\text{opt}}$  can be found and its possible values can be specified in each  
582 case.

583 The results for the different pumping heads show differences between higher and lower  
584 heads. However, there is a power value  $P_e$  above which  $k_{\text{opt}}=0.5$  and the power should be  
585 distributed at 50 % between the two pumps; conversely, if the power is lower than  $P_e$ ,  $k_{\text{opt}}=0$   
586 and all the available power must be assigned to only one of the pumps. But if it exceeds  $P_{\max}$ ,  
587 the power assigned to the pump that is receiving higher power is limited to the value of  $P_{\max}$   
588 and  $k_{\text{opt}} = 1-(P_{\max}/P)$ . This condition occurs only if  $P_e > P_{\max}$  (heads 36, 42 and 48 m).

589 Consequently, there is no power distribution ratio other than 0 and 0.5 that maximises the  
590 flow rate, except that required to limit the power assigned to one of the pumps to  $P_{\max}$ .

591 The determination of the value of  $P_e$  can be established analytically from the curves  
592 representing the flow rate-power relationship of a single pump ( $q(P)$ ), and for the two pumps  
593 in parallel ( $Q(P)$ ) with power distribution of 50 %. Two possibilities can be considered:

594 (a) The curves  $q(P)$  and  $Q(P)$  intersect at a value  $P < P_{\max}$ .

595 (b) The curves  $q(P)$  and  $Q(P)$  do not intersect for values of power  $P < P_{\max}$ .

596 In order to establish the most suitable working strategy for a given set of pumps and a  
597 specific pumping head, it is necessary to determine previously which case applies.

598 In practice, it is possible to determine whether the pumping at a certain head corresponds to  
599 case (a) or (b) using a simple pumping test. Since  $Q(P_{\max})=2q(P_{\max}/2)$ , it is sufficient to carry  
600 out a pumping test with a single pump and to check whether  $q(P_{\max})$  is lower (case a) or  
601 higher (case b) than  $2q(P_{\max}/2)$ .

602 When applying these conclusions to the pumping heads considered in this work, the power  
603 distribution strategy for the lower pumping heads (18, 24 and 30 m) corresponds to case (a)  
604 with  $P_e < P_{\max}$ , while for the higher pumping heads (36, 42 and 48 m) this corresponds to case  
605 (b) with  $P_e > P_{\max}$ .

606 In order to confirm that the conclusions derived from this work can be extrapolated to pumps  
607 of different powers, the same study was conducted with pumps of 1.5 kW, and identical  
608 results were obtained.

609 The proposed methodology can probably be generalised to pumping groups with higher  
610 numbers of pumps in parallel.

611 Further work is in progress related to the application of the method for distributing the power  
612 generated in the PV system proposed in this paper from the modelling of the facility during a  
613 whole year.

614

## 615 **6. References**

616 Aliyu, M., Hassan, G., Said, S.A., Siddiqui, M.U., Alawami, A.T., 2018. A review of solar-  
617 powered water pumping systems. *Renew. Sust. Energ. Rev.* 87, 61-76.

618 Almeida, R.H.; Carrêlo, I.B.; Lorenzo, E.; Narvarte, L.; Fernández-Ramos, J.; Martínez-  
619 Moreno, F.; Carrasco, L.M., 2018a. Development and Test of Solutions to Enlarge the Power  
620 of PV Irrigation and Application to a 140 kW PV-Diesel Representative Case. *Energies* 11,  
621 3538.

622 Almeida, R.H., Ledesma, J.R., Carrêlo, I.B., Narvarte, L., Ferrara, G., Antipodi, L., 2018b. A  
623 new pump selection method for large-power PV irrigation systems at a variable frequency,  
624 *Energ. Convers Manage.* 174, 874-885.

625 Alonso, M., 2005. *Sistemas fotovoltaicos. Introducción al diseño y dimensionado de*  
626 *instalaciones de energía solar fotovoltaica.* S.A.P.T. Publicaciones técnicas SL.

627 Alonso, M., Lorenzo, E., Chenlo, F., 2003. PV water pumping systems based on standard  
628 frequency converters. *Prog. Photovolt.: Res. Appl.* 11, 179-191.

629 Benghanem, M., Daffallah, K.O., Almohammed, A., 2018. Estimation of daily flow rate of  
630 photovoltaic pumping systems using solar radiation data. *Results Phys.* 8, 949-954.

631 Benlarbi, K., Mokrani, L., Nait-Said, M.S., 2004. A fuzzy global efficiency optimization of a  
632 photovoltaic water pumping system. *Sol. Energy* 77, 203-216.

633 Bione, J., Vilela, O.C., Fraidenaich, N., 2004. Comparison of the performance of PV water  
634 pumping systems driven by fixed, tracking and V-trough generators. *Sol. Energy* 76: 703-  
635 711.

636 *Bombas Ideal Catalogue. SKI Series.* [www.bombasideal.com/wp-](http://www.bombasideal.com/wp-content/uploads/2018/07/Catalogo-SUM-1078.compressed.pdf)  
637 [content/uploads/2018/07/Catalogo-SUM-1078.compressed.pdf](http://www.bombasideal.com/wp-content/uploads/2018/07/Catalogo-SUM-1078.compressed.pdf) [accessed 29 July 2019].

638 Campana, P.E., Li, H., Yan, J., 2013. Dynamic modelling of a PV pumping system with  
639 special consideration on water demand. *Appl. Energ.* 112, 635-645.

640 Carrêlo, I.B., Almeida, R.H., Narvarte, L., Martínez-Moreno, F., Carrasco, L.M., 2020.  
641 Comparative analysis of the economic feasibility of five large-power photovoltaic irrigation  
642 systems in the Mediterranean region. *Renew. Energ.* 145, 2671-268.

643 Elkholy, M.M., Fathy, A., 2016. Optimization of a PV fed water pumping system without  
644 storage based on teaching-learning-based optimization algorithm and artificial neural network  
645 *Sol. Energy* 139, 199-212.

646 Espericueta, A.D.C., Foster, R.E., Ross, M.P., Hanley, C., Gupta, V.P., Avilez, O.M., Rubio,  
647 A.R.P., 2004. Ten-Year Reliability Assessment of Photovoltaic Water Pumping Systems in  
648 Mexico, in *Solar 2004*; American Solar Energy Society: Portland, OR, USA.

649 Fedrizzi, M.C., Sauer, I.L., 2002. Bombeamento Solar Fotovoltaico, Histórico, Características  
650 e Projectos. In Encontro de Energia no Meio Rural; SciELO: Campinas, Brazil.

651 García-Tejero, I.F., Durán-Zuazo, V.H. (Eds.), 2018. Water scarcity and sustainable  
652 agriculture in semiarid environment. Tools, strategies and challenges for woody crops. 1st  
653 Ed. Academic Press.

654 Guzmán, A.B., Vicencio, R.B., Ardila-Rey, J.A., Ahumada, E.N., Araya, A.G., Moreno, G.A.,  
655 2018. A Cost-Effective Methodology for Sizing Solar PV Systems for Existing Irrigation  
656 Facilities in Chile. *Energies* 11, 1853.

657 Hamrouni, N., Jraid, M., Chérif, A., 2009. Theoretical and experimental analysis of the  
658 behaviour of a photovoltaic pumping system. *Sol. Energy* 83, 1335-1344.

659 IEC 62253:2011. Photovoltaic pumping systems – Design qualification and performance  
660 measurements. International Electrotechnical Commission,  
661 <https://webstore.iec.ch/publication/6636> [accessed 29 July 2019].

662 Kaya, D., Yagmur, E.A., Yigit, K.S., Kilic, F.C., Eren, A.S., Celik, C., 2008. Energy efficiency  
663 in pumps. *Energ. Convers. Manage.* 49, 1662-1673.

664 Koor, M., Vassiljev, A., Koppel, T., 2016. Optimization of pump efficiencies with different  
665 pumps characteristics working in parallel mode. *Adv. Eng. Softw.* 101, 69-76.

666 López-Luque, R., Reza, J., Martínez, J., 2015. Optimal design of a standalone direct  
667 pumping photovoltaic system for deficit irrigation of olive orchards. *Appl. Energ.* 149, 13-23.

668 Matam, M., Barry, V.R., Govind, A.R., 2018. Optimized Reconfigurable PV array based  
669 Photovoltaic water-pumping system *Sol. Energy* 170, 1063-1073.

670 Meah, K., Fletcher, S., Ula, S., 2008. Solar photovoltaic water pumping for remote locations.  
671 *Renew. Sust. Energ. Rev.* 12, 472-487.

672 Mérida García, A., Fernández García, I., Camacho Poyato, E., Montesinos Barrios, P.,  
673 Rodríguez Díaz, J.A., 2018. Coupling irrigation scheduling with solar energy production in a  
674 smart irrigation management system. *J. Clean. Prod.* 175, 670-682.

675 Narvarte, L., Fernández-Ramos, J., Martínez-Moreno, F., Carrasco, L.M., Almeida, R.H.,  
676 Carrêlo, I.B., 2018. Solutions for adapting photovoltaics to large power irrigation systems for  
677 agriculture. *Sustainable Energy Technologies and Assessments* 29, 119-130.

678 Pemberton, M., Bachmann, J., 2010. Pump systems performance impacts multiple bottom  
679 lines. *Coal Age* 115, 46-48.

680 Shankar, A., Kalaiselvan, V., Subramaniam, U., Shanmugam, P., 2016. A comprehensive  
681 review on energy efficiency enhancement initiatives in centrifugal pumping system. *Appl.*  
682 *Energ.* 181, 495-513.

683 Shoeb, M.A., Shafiullah, G., 2018. Renewable Energy Integrated Islanded Microgrid for  
684 Sustainable Irrigation—A Bangladesh Perspective. *Energies* 11, 1283.

685 Talbi, B., Krim, F., Rekioua, T., Mekhilef, S., Laib, A., Belaout, A., 2018. A high-performance  
686 control scheme for photovoltaic pumping system under sudden irradiance and load changes  
687 *Sol. Energy* 159, 353-368.

- 688 Tiwari, A.K., Kalamkar, V.R., 2018. Effects of total head and solar radiation on the  
689 performance of solar water pumping system. *Renew. Energ.* 118, 919-927.
- 690 Todde, G., Murgia, L., Deligios, P.A., Hogan, R., Carrelo, I., Moreira, M., Pazzona, A., Ledda,  
691 L., Narvarte, L., 2019. Energy and environmental performances of hybrid photovoltaic  
692 irrigation systems in Mediterranean intensive and super-intensive olive orchards. *Sci. Total*  
693 *Environ.* 651, 2514-2523.
- 694 Wazed, S.M., Hughes, B.R., O'Connor, D., Calautit, J.K., 2018. A review of sustainable solar  
695 irrigation systems for Sub-Saharan Africa. *Renew. Sust. Energ. Rev.* 81, 1206-1225.
- 696
- 697